Discovery of Year-Scale Time Variabilities of Thermal and Non-Thermal X-ray Emission in Tycho's Supernova Remnant

M. Matsuda (Kyoto U.)

matsuda.masamune.38a@st.kyoto-u.ac.jp

H. Uchida, T. G. Tsuru (Kyoto U.), T. Tanaka (Konan U.), H. Yamaguchi (ISAS/JAXA, UTokyo)

EAS 2022 (June 27th – July 1st, 2022)

Valencia Conference Centre, Spain

Tycho’s SNR

Movie made from Chandra images

0.5–1.5 keV
1.6–2.3 keV
4.1–6.1 keV

A.D. 2003→ 2007→ 2009 → 2015

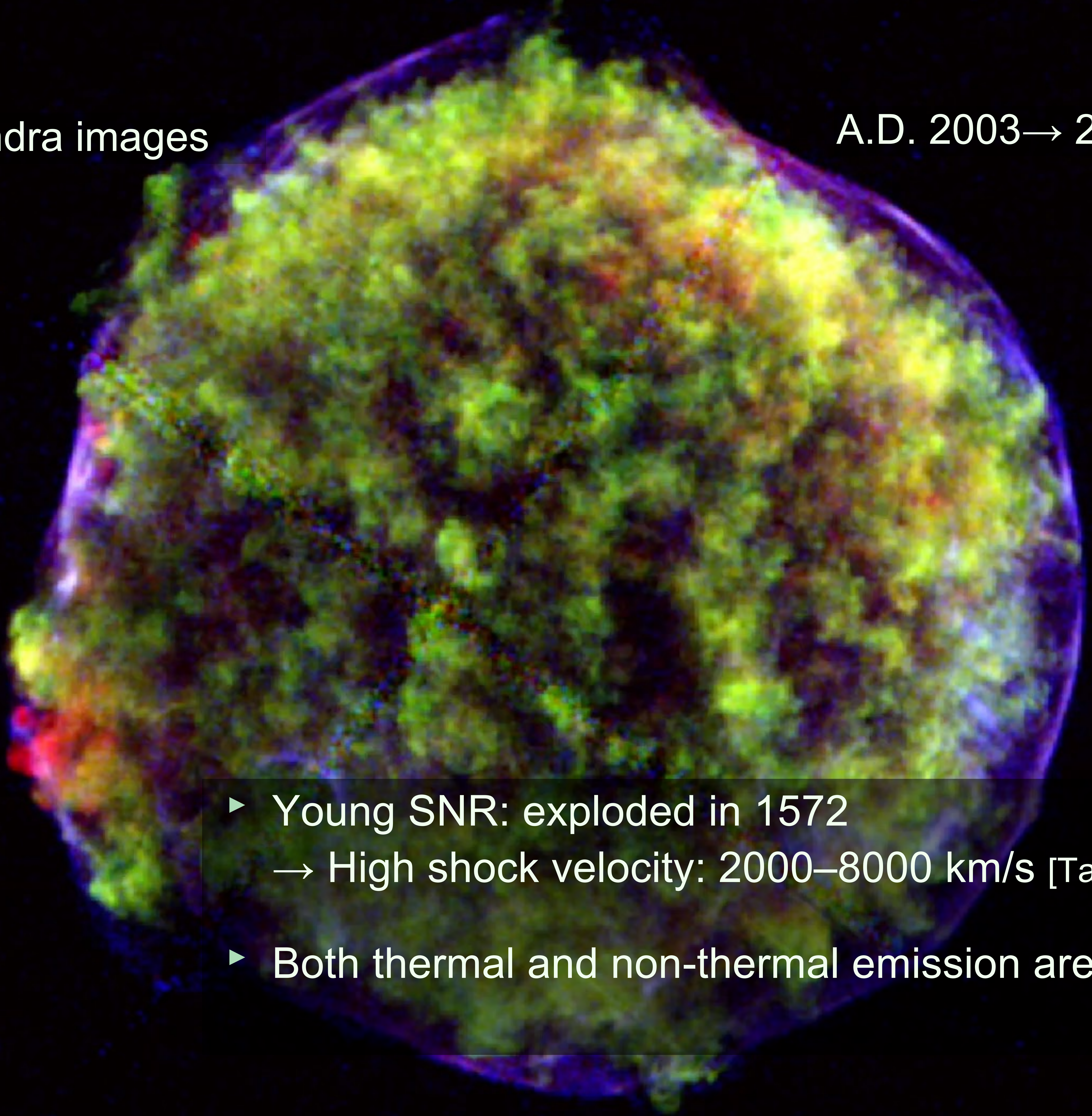

~3 pc

- Young SNR: exploded in 1572
  → High shock velocity: 2000–8000 km/s [Tanaka+ 2021]
- Both thermal and non-thermal emission are bright [Hwang+ 2002]

Non-thermal X-ray Time-Variabilities in Tycho's SNR

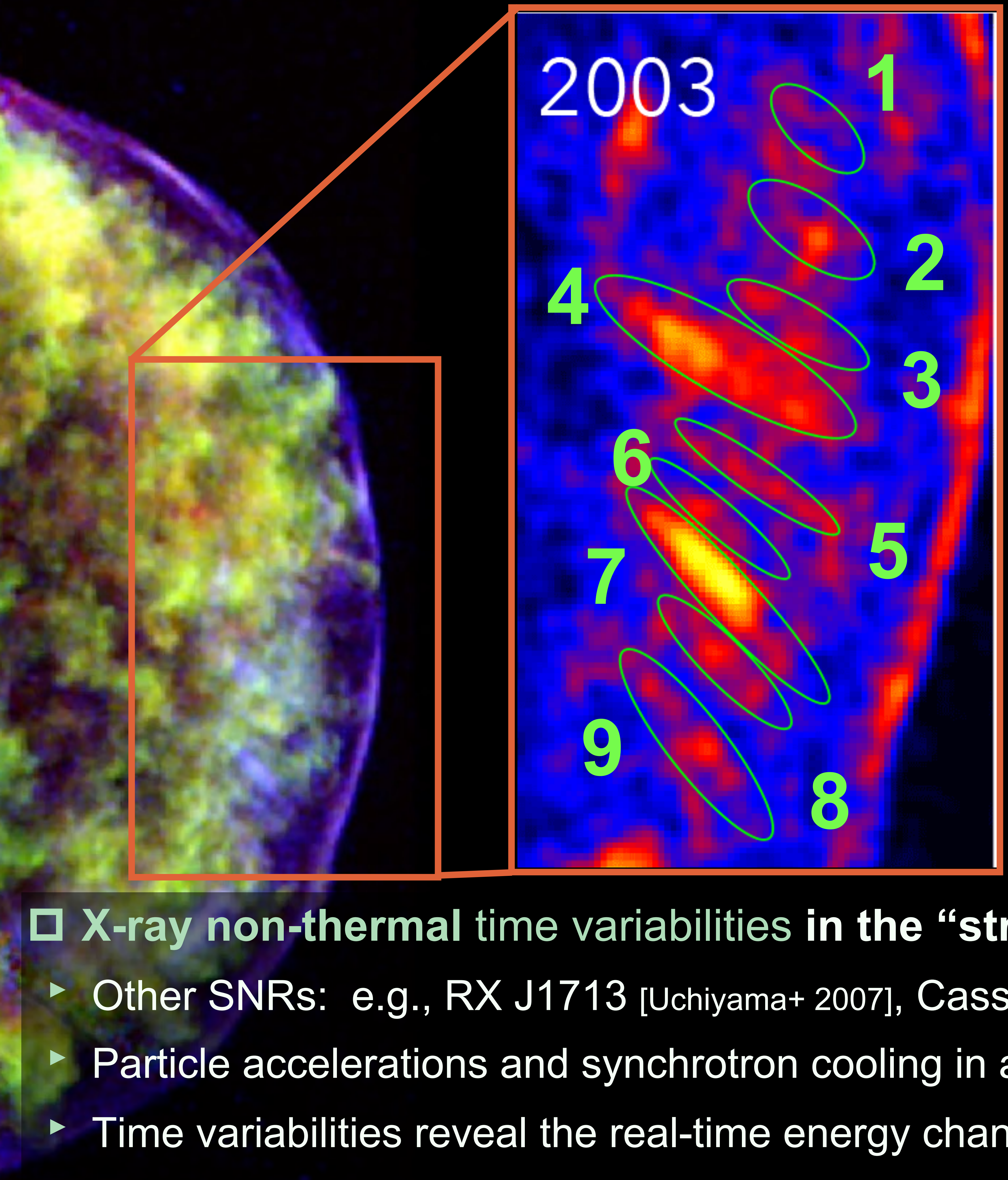

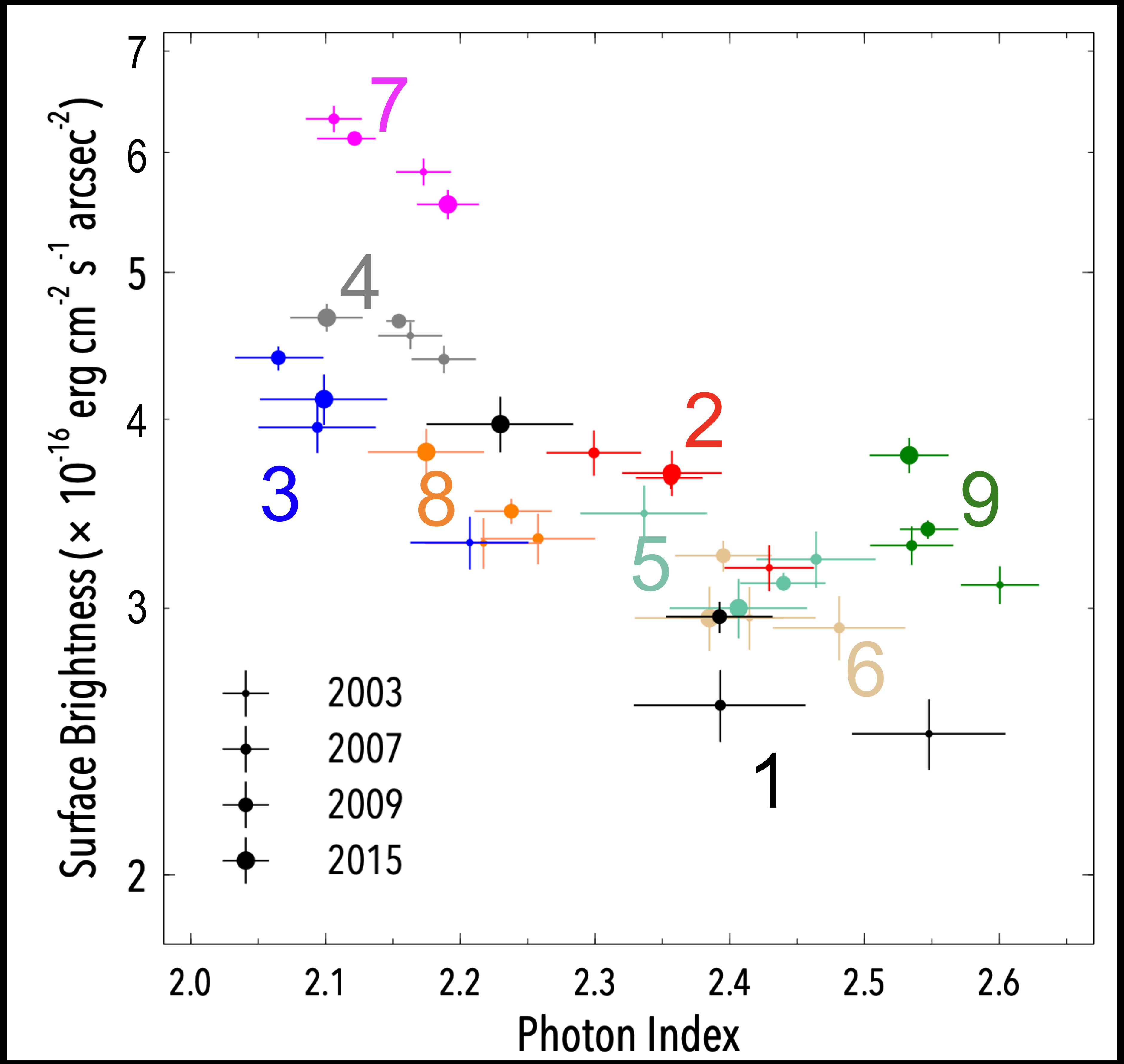

- **X-ray non-thermal** time variabilities **in the "stripe" region (Okuno, MM+ 2020; MM+ 2020)**
  - Other SNRs: e.g., RX J1713 [Uchiyama+ 2007], Cassiopeia A [Uchiyama & Aharonian 2008], G330.2+1.0 [Borkowski+ 2018]
  - Particle accelerations and synchrotron cooling in amplified magnetic field (?)
  - Time variabilities reveal the real-time energy change of particles.

→ How about **Thermal X-ray**?

Thermal X-ray Time-Variabilities

Thermal X-ray time-variabilities

- There are few examples of X-ray time-variabilities (e.g., Cassiopeia A: Patnaude & Fesen 2007)
- It will be a hint of solving the problem of the electron heating mechanism.

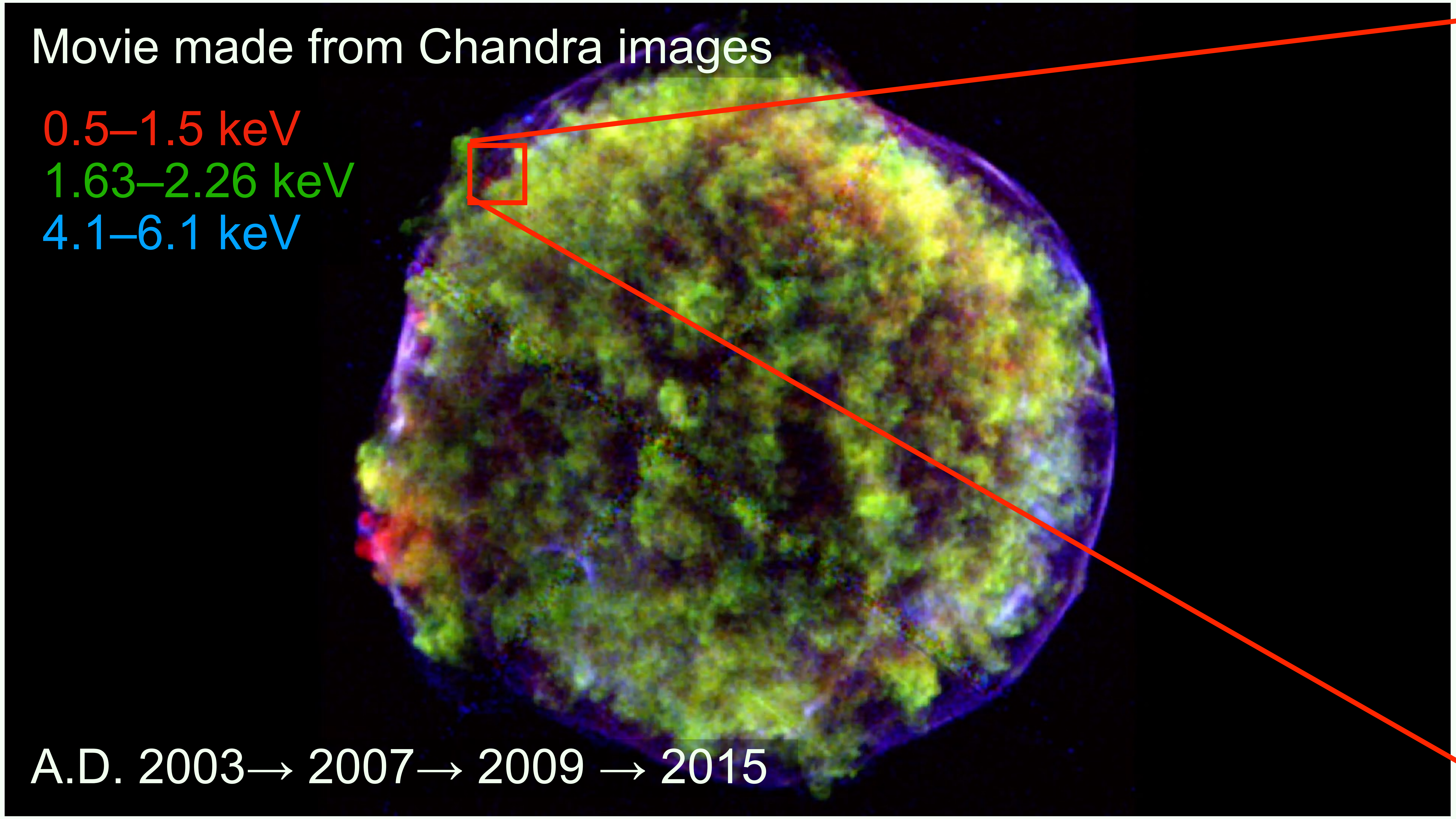

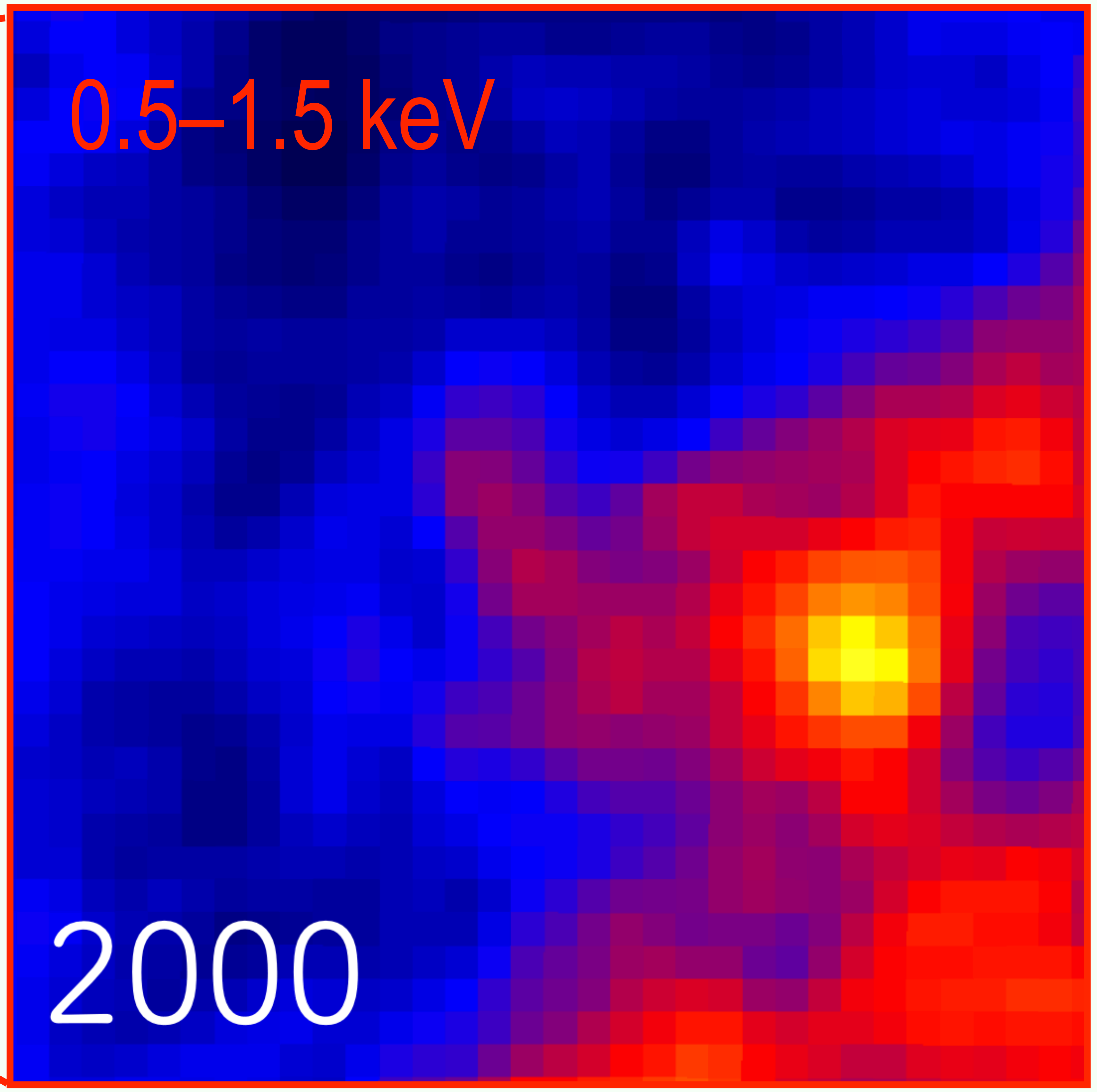

First discovery of thermal X-ray brightening in Tycho (MM+, submitted to ApJ)

Spectra of Time Variable Region (Knot1) and Nearby Region (Ref1)

- Knot1 is brighter than Ref1 in $\lesssim$ 1.5 keV band.
- The energy band with the high Knot1/Ref1 ratio expands to higher energy year by year.

Fitting Results

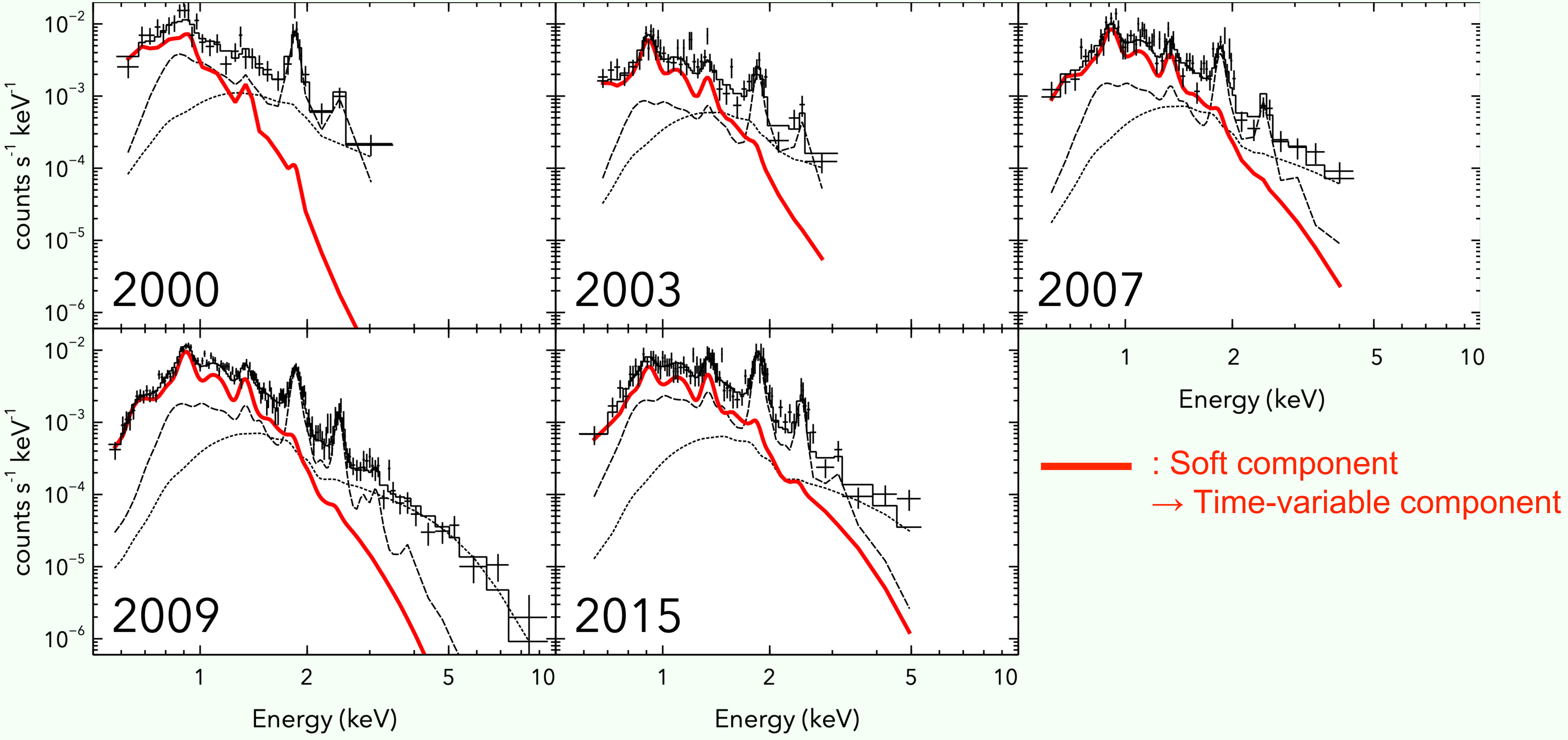

- The contribution of the soft component changes year by year (discussed later).
- The soft component with the solar abundance can explain the spectra.

Comparison with Hα Images in Knot1

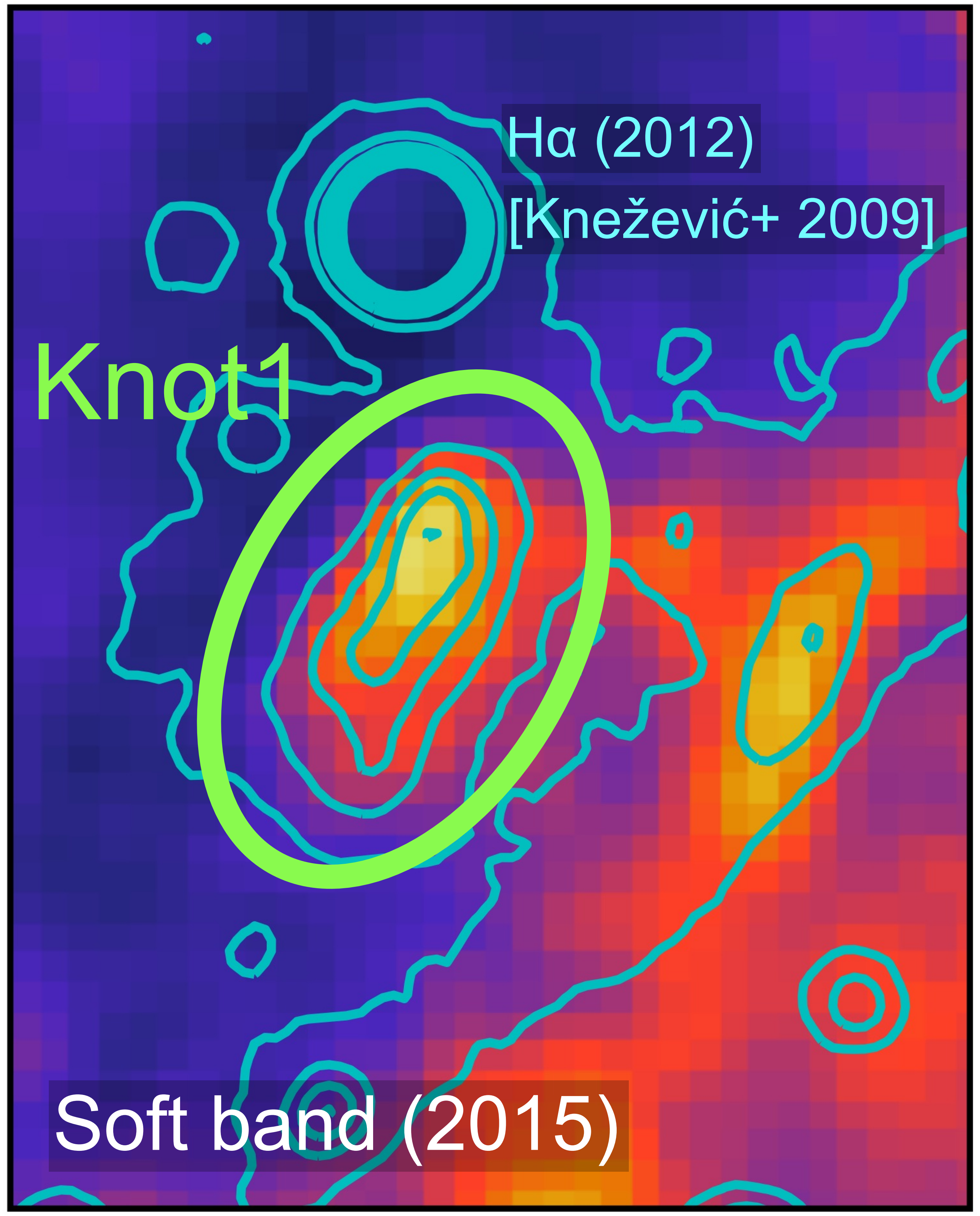

Hα line images have good correlation with Knot1.

Interaction between forward shock and neutral H gas

[Ghavamian+ 2000]

Strong evidence that Knot1 originates from ISM (First detection in Tycho)

Best-Fit Parameters of the Soft Component

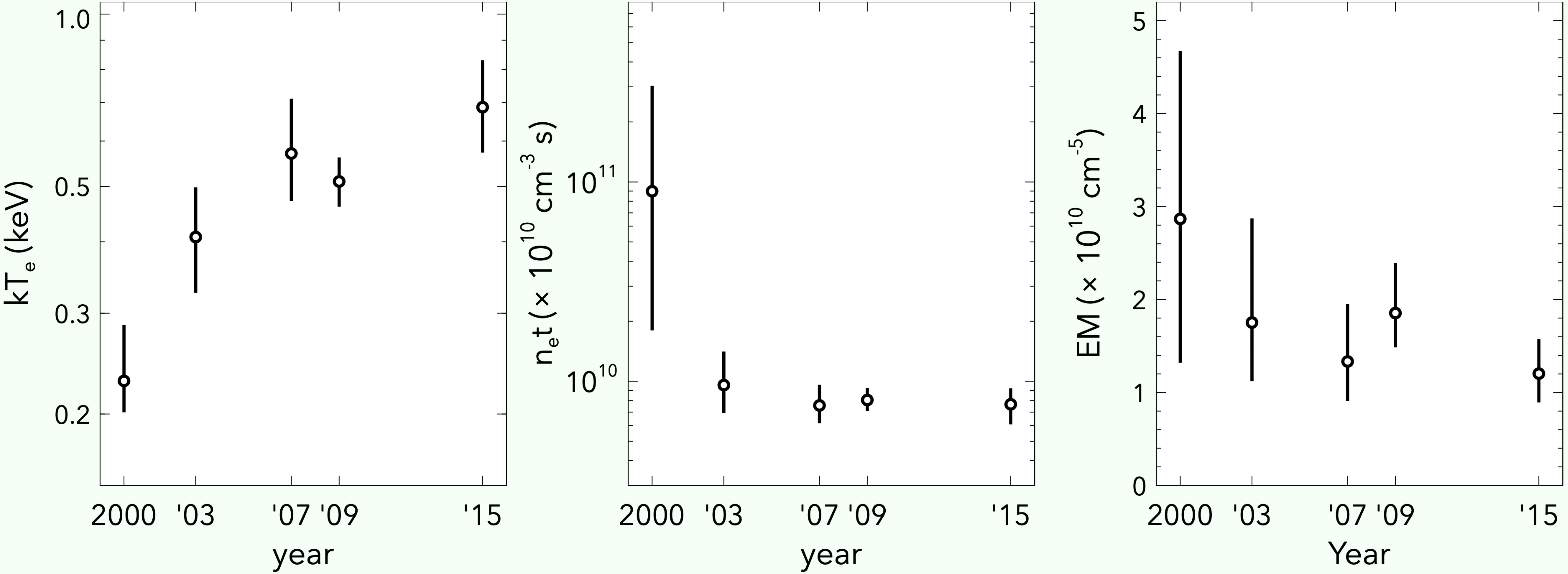

- Density of Knot1 is estimated as ~10 cm^{-3} from Emission Measures ($n_e n_{\mathrm{H}} V / 4\pi d^2$).
  (cf. Densities near Knot1 is 0.3–1.0 cm^{-3} [Williams+ 2013])
  - Knot1 is about 10 times denser than its surroundings
- kT_e increased from ~0.2 keV to ~0.7 keV in 15 years.

The Interpretation of the Increase of kT_e

Proton Temperature

$$kT_{p,\mathrm{init}} = \frac{3}{16} m_p v_{\mathrm{sh}}^2$$

Electron temperature

Collisionless Electron heating

$$kT_{e,\mathrm{init}} = \beta_0 kT_{p,\mathrm{init}}$$
$$(\beta_0 = 0.05)$$

Only Coulomb collisions

$$kT_{e,\mathrm{init}} = \frac{3}{16} m_e v_{\mathrm{sh}}^2$$
$$(\beta_0 = m_e/m_p)$$

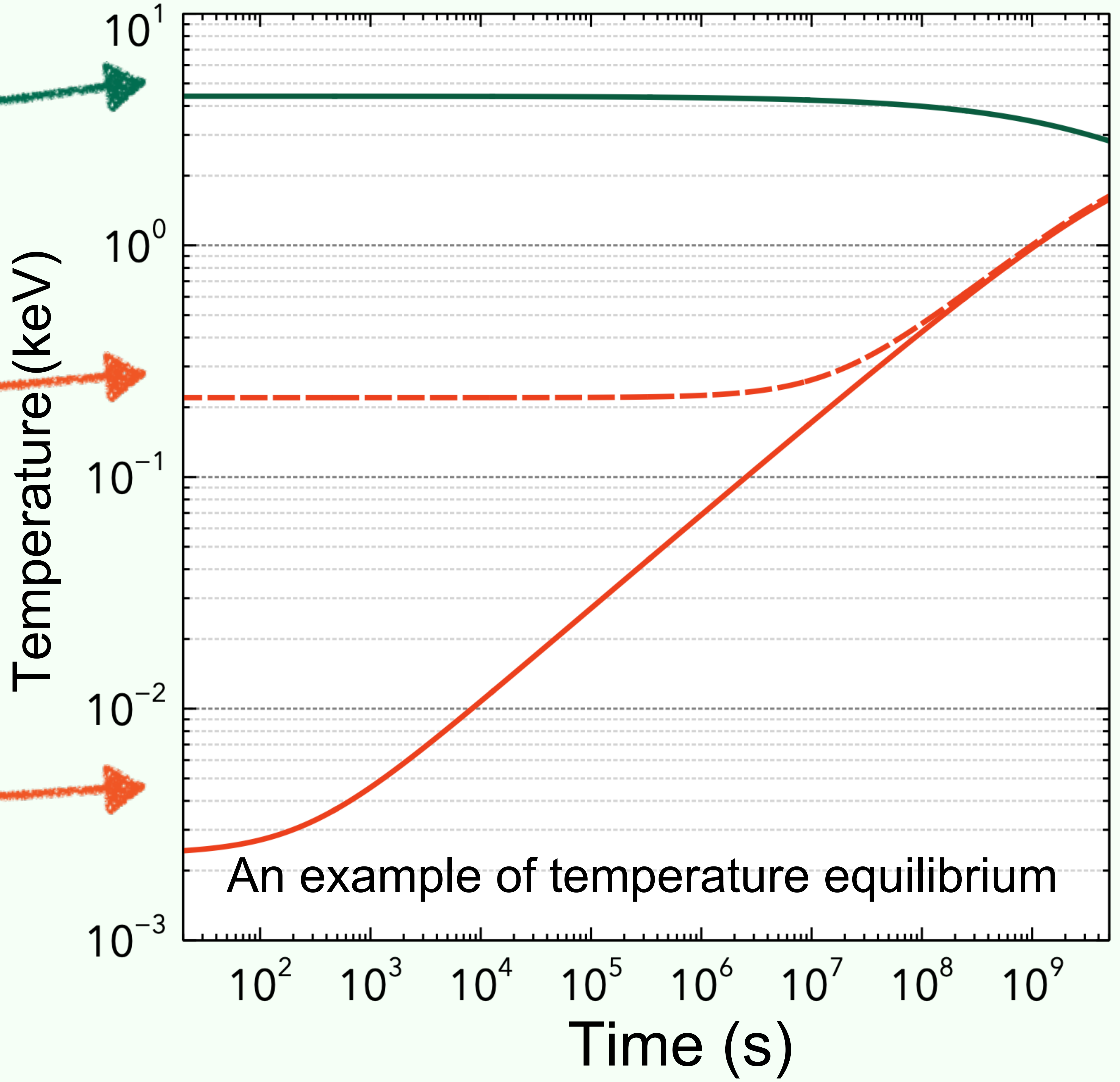

- β_0 represents the efficiency of collisionless heating at the shock transition.
- We compared the observed kT_e increase from the calculations for different β_0.

Comparison with the Observation and Calculation

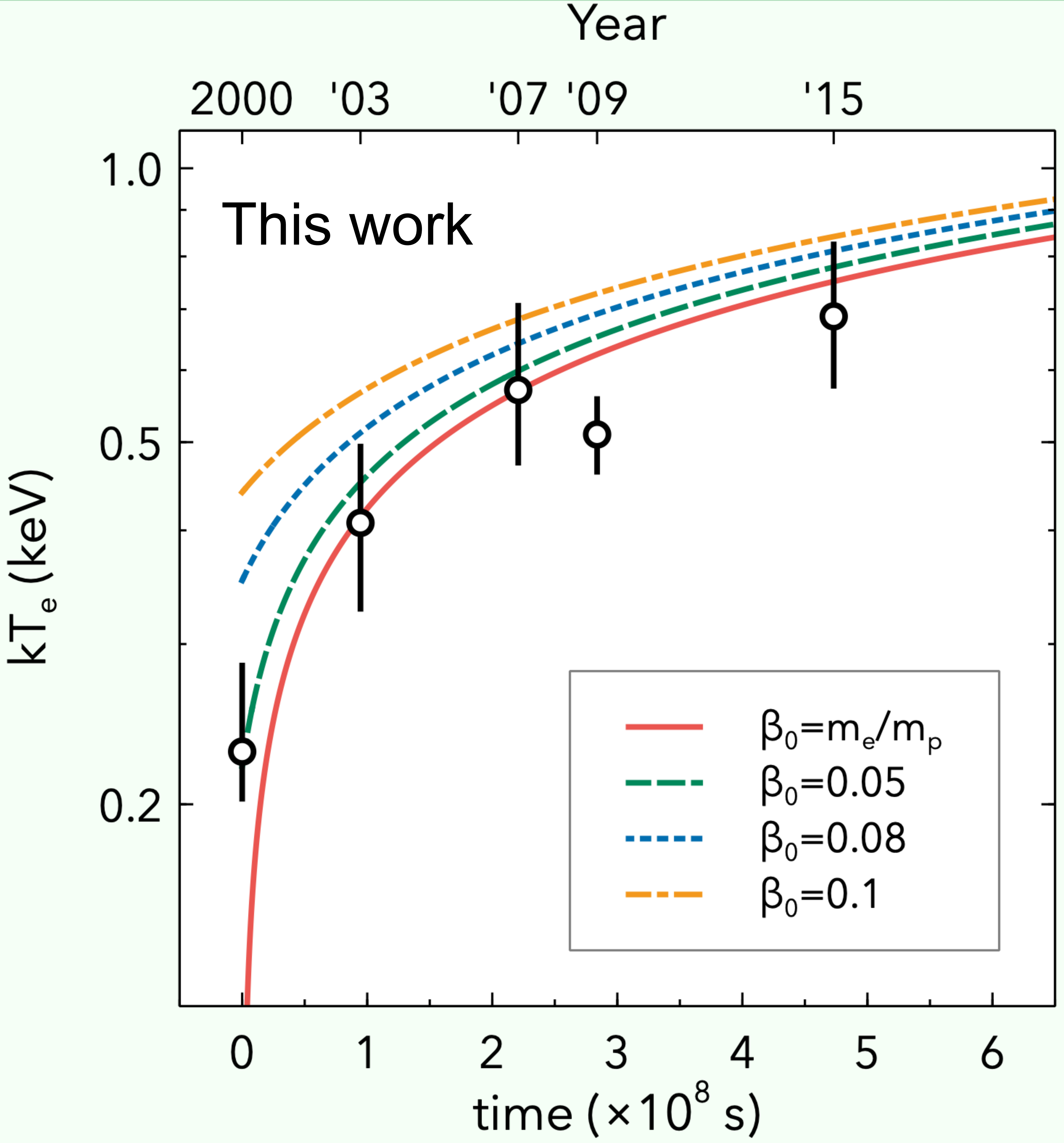

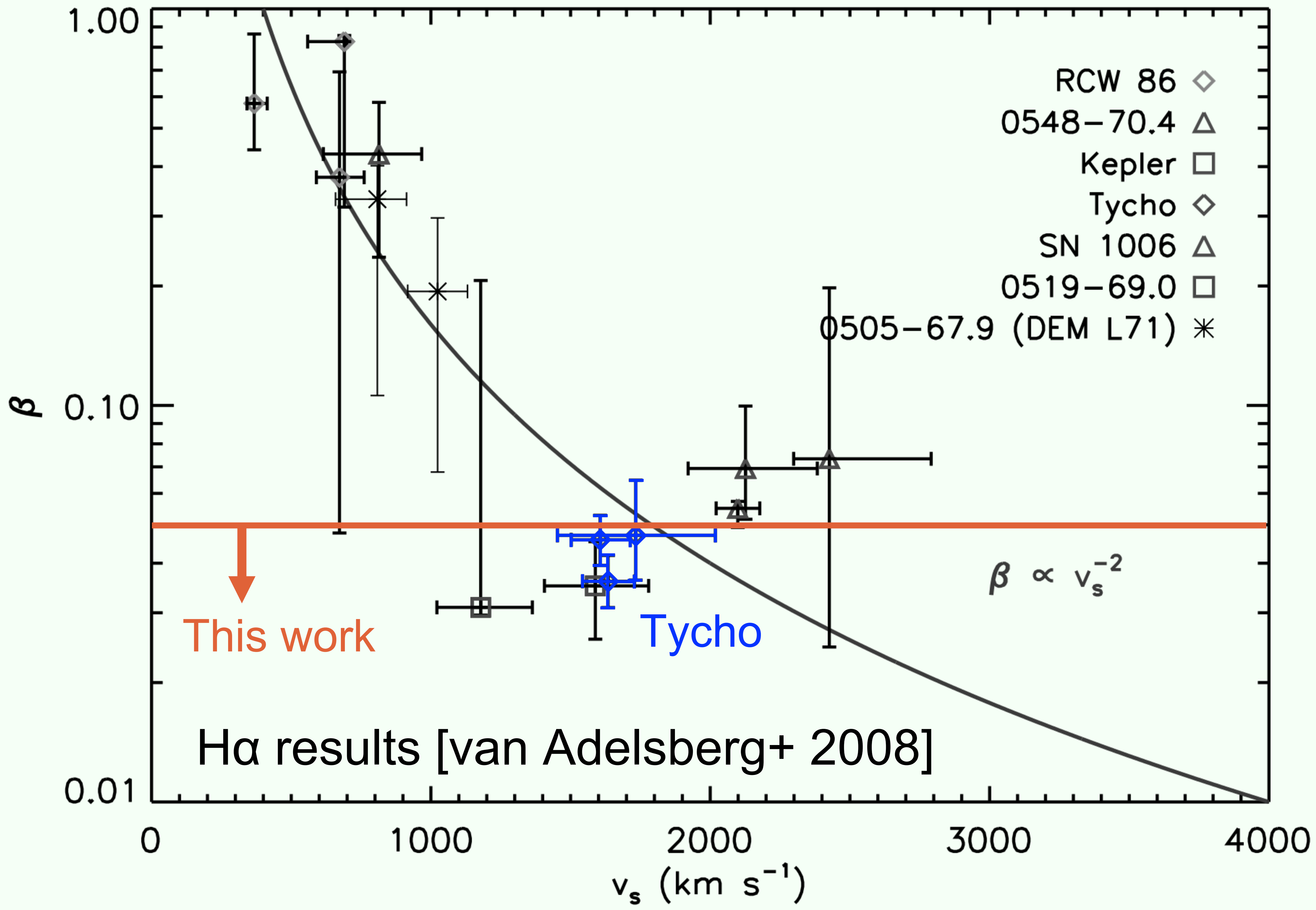

- β_0 is required to be $m_e/m_p \lesssim \beta_0 \lesssim 0.05$ to reproduce the observed kT_e change.
- This result is consistent with Hα results.

Conclusion

- We analyzed time variabilities in Tycho's SNR
- Discovery of thermal-Xray time-variabilities
  - Originated from ISM/CSM (First detection in Tycho's SNR)
  - Electron heating was observed in the region
- We presented a method for estimating the collisionless heating efficiency independently of Hα observations.

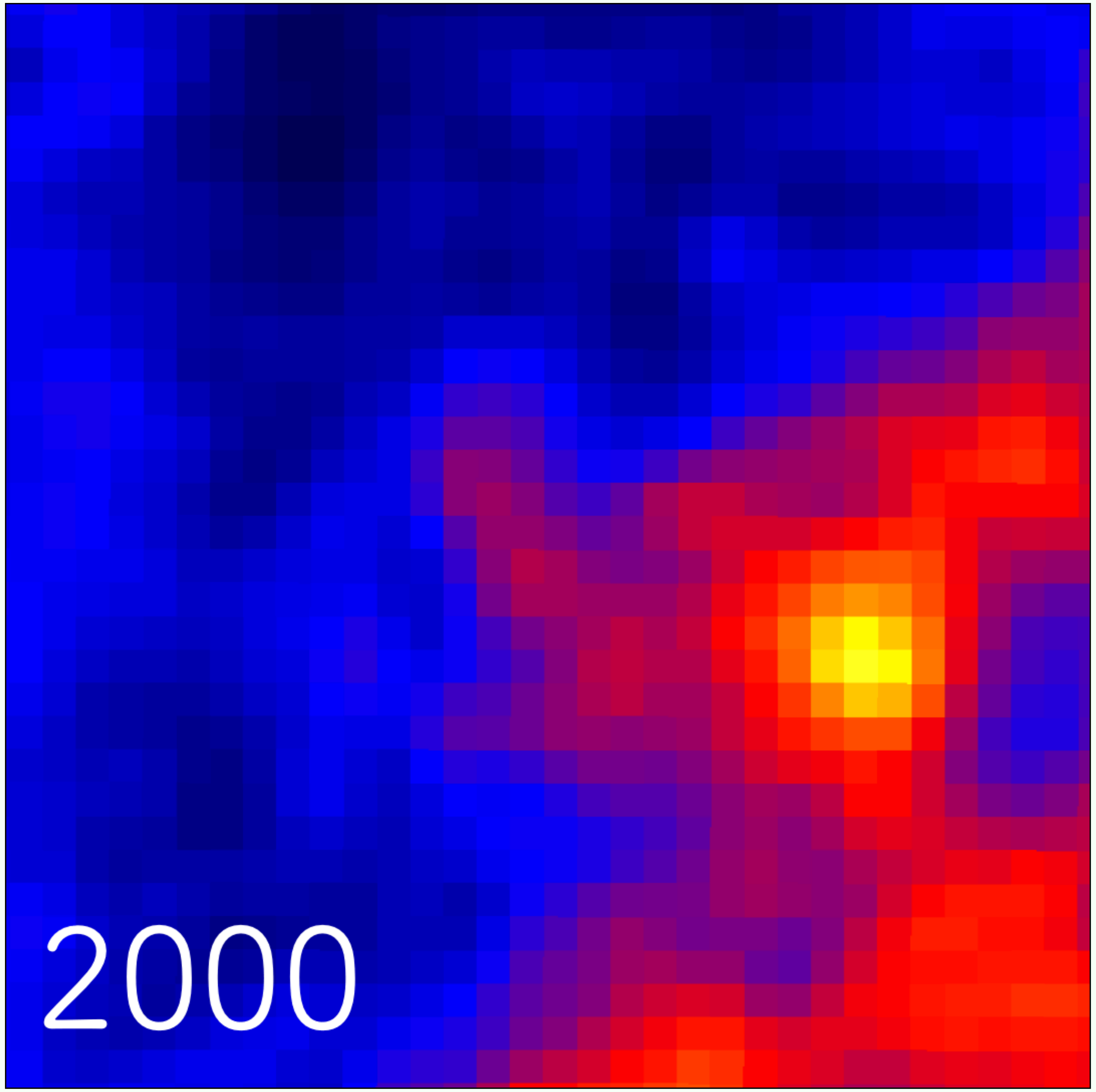

Backup

Correlation between stripe and ISM

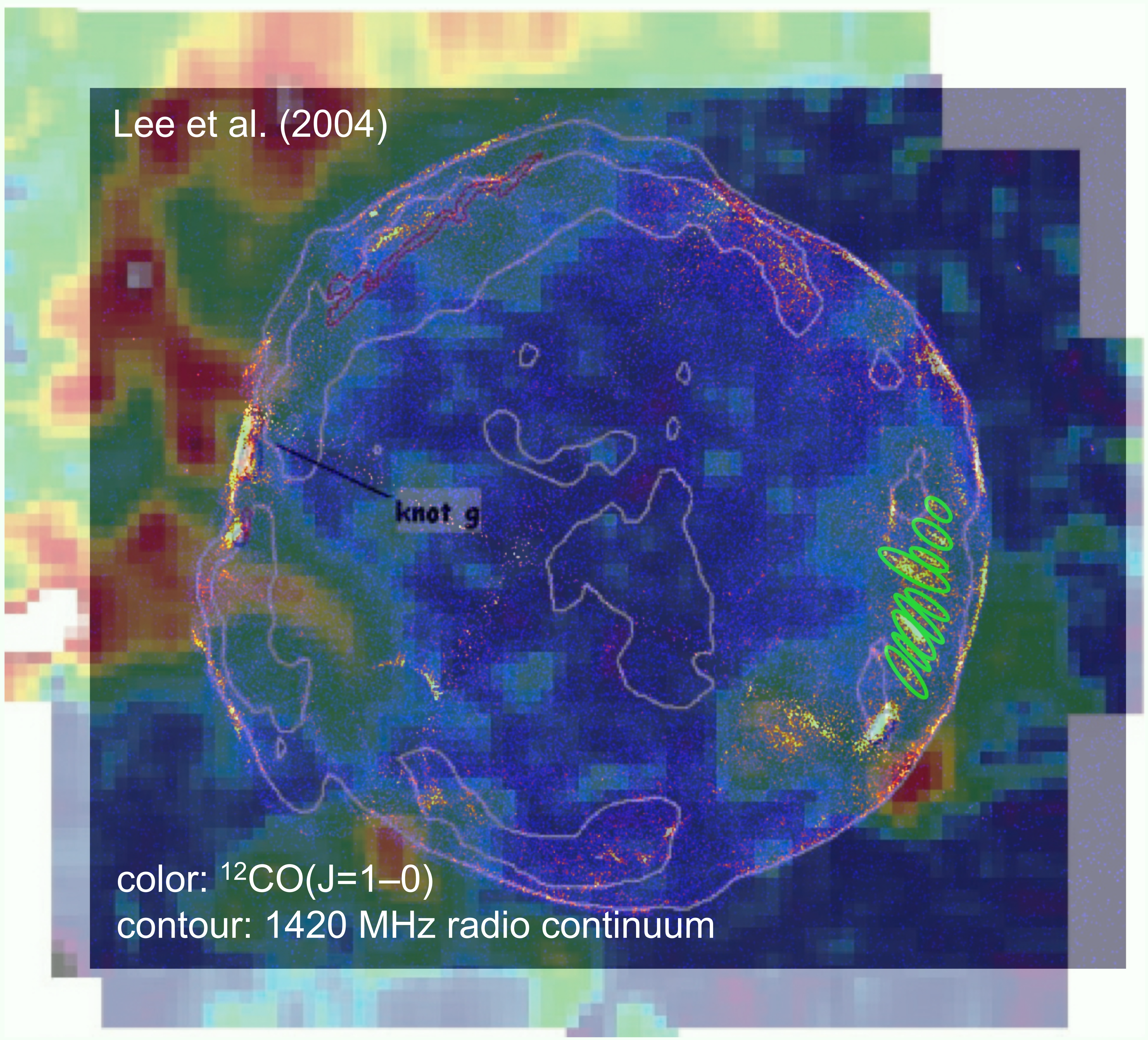

Williams+13

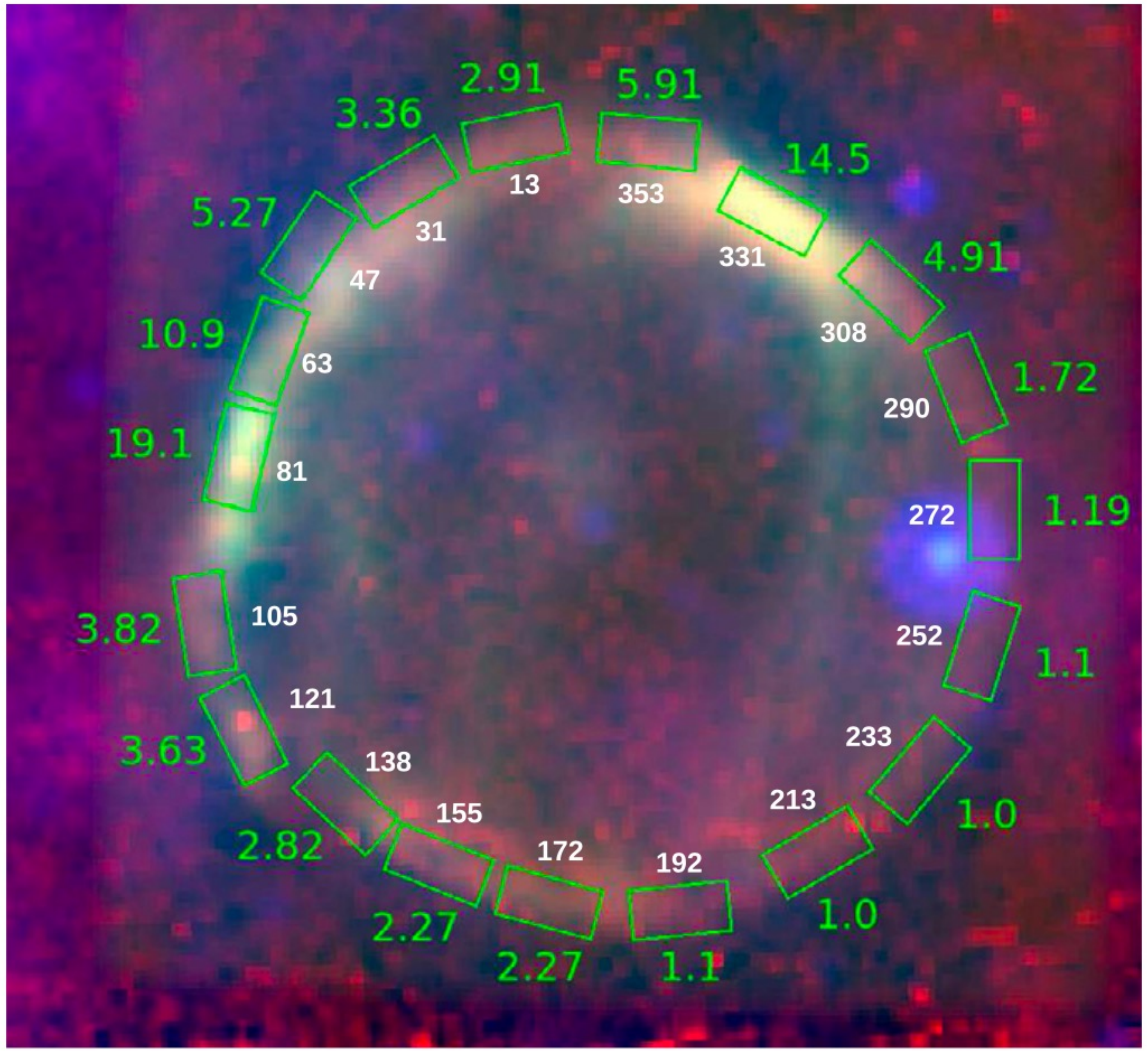

Figure 2. The normalized post-shock density in various regions of Tycho, along with outlines of the spatial regions used for our analysis, superposed on a three-color IR image, with *Spitzer* 70 μm emission in red, 24 μm emission in green, and *WISE* 12 μm in blue. North is up and east is to the left. The absolute scaling for the densities are 0.11 for the compact grain model and 0.2 for the porous grain model (see Section 4.4 and Table 2 for details). Interior numbers are azimuthal angle, in degrees.

(A color version of this figure is available in the online journal.)

Table 2
Results

Deg.	Density (cm^{-3})	Pressure (dyne cm^{-2})
13	$0.32^{0.40}_{0.27}$	$2.51^{3.16}_{2.01} \times 10^{-8}$
32	$0.37^{0.46}_{0.31}$	$2.37^{2.99}_{1.90} \times 10^{-8}$
47	$0.58^{0.72}_{0.48}$	$1.89^{2.38}_{1.52} \times 10^{-8}$
63	$1.2^{1.5}_{1.0}$	$2.59^{3.39}_{1.92} \times 10^{-8}$
81	$2.1^{2.6}_{1.7}$	$6.00^{7.77}_{4.55} \times 10^{-8}$
105	$0.42^{0.52}_{0.35}$	$2.37^{2.99}_{1.90} \times 10^{-8}$
121	$0.4^{0.50}_{0.33}$	$2.88^{3.62}_{2.31} \times 10^{-8}$
138	$0.31^{0.38}_{0.26}$	$2.00^{2.52}_{1.61} \times 10^{-8}$
155	$0.25^{0.31}_{0.21}$	$1.77^{2.28}_{1.36} \times 10^{-8}$
172	$0.25^{0.31}_{0.21}$	$1.53^{1.97}_{1.18} \times 10^{-8}$
192	$0.12^{0.15}_{0.10}$	$1.00^{1.26}_{0.80} \times 10^{-8}$
213	$0.11^{0.14}_{0.09}$	$1.06^{1.36}_{0.81} \times 10^{-8}$
233	$0.11^{0.14}_{0.09}$	$1.02^{1.29}_{0.82} \times 10^{-8}$
252	$0.12^{0.15}_{0.10}$	$1.08^{1.39}_{0.82} \times 10^{-8}$
272	$0.13^{0.16}_{0.11}$	$1.13^{1.42}_{0.91} \times 10^{-8}$
290	$0.19^{0.24}_{0.16}$	$1.52^{1.92}_{1.22} \times 10^{-8}$
308	$0.54^{0.67}_{0.45}$	$4.05^{5.10}_{3.25} \times 10^{-8}$
331	$1.6^{2.0}_{1.3}$	$9.58^{12.1}_{7.69} \times 10^{-8}$
353	$0.65^{0.81}_{0.54}$	$2.15^{2.71}_{1.73} \times 10^{-8}$

Notes. Densities are post-shock. Pressure calculation assumes compression ratio of 4 at the shock front. Both assume standard ISM dust grain models of Weingartner & Draine (2001) and $D = 2.3$ kpc (see the text for details of dependence on these quantities).